Available online at www.sciencedirect.com

ScienceDirect

journal homepage: http://www.elsevier.com/locate/rpor

Original research article

Estimation of peripheral dose from Co^{60} beam in water phantom measured in Secondary Standard Dosimetry Laboratory, Pakistan

Muhammad Shahban[a,*], *Babar Hussain*[b], *Khalid Mehmood*[b], *Shakeel Ur Rehman*[c]

[a] *Nuclear Medicine, Oncology and Radiotherapy Institute, Nawabshah, Pakistan*
[b] *Pakistan Institute of Nuclear Science and Technology (PINSTECH), Islamabad, Pakistan*
[c] *Pakistan Institute of Engineering and Applied Sciences (PIEAS), Islamabad, Pakistan*

ARTICLE INFO

Article history:
Received 14 July 2016
Received in revised form
14 October 2016
Accepted 20 December 2016
Available online 21 April 2017

Keywords:
Co^{60} beam
Peripheral dose
Water phantom
SSDL

ABSTRACT

Background: Peripheral or scatter dose harms neighbouring normal tissues during administration of dose to cancerous tissues, therefore, knowledge of peripheral dose is an important consideration in radiotherapy.
Aim: In present study, absorbed dose measurements in a water phantom were performed for three field sizes, $7 \times 7\,cm^2$, $10 \times 10\,cm^2$ and $15 \times 15\,cm^2$.
Materials and methods: For each field size, dose was measured at six depths below the front surface of the water phantom; 2.5–15 cm with an interval of 2.5 cm. Measurements were made at equal transverse distances along the horizontal axis, from 1 cm to 6 cm, on both sides of the central beam axis and normalized with central axis dose of each field. All measurements were made at the source to surface distance of 100 cm.
Results: Variation of peripheral dose with lateral distance was analysed and an appropriate parametric equation for each field size and depth was constructed.
Conclusions: The peripheral radiation dose showed a strong dependence on field size and distance from field boundary.

1. Background and aim

Radiotherapy has long been used as cancer treatment modality but with associated risk of producing complications in normal tissues. It has been proven before in near and distant past by many authors[1–13] that there exists a significant unavoidable dose, called peripheral dose or scattered dose, to the organs outside the target volume being treated by a radiation beam of a certain field size. This peripheral dose is due to the scattered radiation coming from the machine head and patient (or phantom), shielding and walls or ceiling of the room.[10] It can cause cataract, damage fertility and can be a great danger for a foetus in pregnant patients. Fraass

* *Corresponding author.*
E-mail address: shahban_butt@yahoo.com (M. Shahban).
http://dx.doi.org/10.1016/j.rpor.2016.12.002

et al.[2] cited BIER III report which summarizes the threshold dose values for different organs, like breast, lungs, thyroid, gonads and foetus in pregnant women. A single fraction of more than 10 cGy can induce serous foetus damage. Above the threshold of 100 cGy, there is an increase in cancer probability of about 0.5%/cGy of dose delivered in breast of women above twenty years of age. Single fraction of more than 300 cGy can cause sterility in males. For thyroid and lungs cancers, possible threshold can be set at a safe limit of 5 cGy. If patient is treated with prescribed dose of 50–60 Gy, these threshold doses correspond to less than 3% of the prescribed dose.[2] Prior knowledge of this scattered radiation is therefore extremely important to gain best possible ratio between Tumor Control Probability (TCP) and Normal Tissue Complication probability (NTCP).[1] It is the main responsibility of the medical physicist to accurately assess this unavoidable dose to make radiotherapy treatment as efficient and safe as possible.

2. Materials and methods

All measurements were performed in the Secondary Standard Dosimetry Laboratory (SSDL), Pakistan. A Co^{60} tele-therapy unit model GWGP-80 was used to produce collimated beam of gamma radiation. The absorbed radiation dose was measured in a PMMA water phantom of dimension 30 cm × 30 cm × 30 cm at SSD of 100 cm. A 0.62 cm^3 A19 Farmer type thimble ion chamber serial number XAQ082331 in conjunction with max-4000 electrometer serial no. F082272 was used for dose measurements. The chamber was positioned in a PMMA inserter sleeve and aligned using a laser system. Peripheral doses were measured for the field sizes 7 × 7 cm^2, 10 × 10 cm^2 and 15 × 15 cm^2 defined at the front phantom surface. For each field size, dose was measured at six depths in water, 2.5–15 cm with an interval of 2.5 cm, at equal transverse distances, from 1 cm to 6 cm, on both sides of the central beam axis. The transverse distance step of 1 cm was chosen. For each field size, dose readings were normalized against central axis dose (approximately un-scattered dose) at the quoted depth and field size. All measurements were made at the source to surface distance (SSD) of 100 cm. Fig. 1 is a schematic diagram depicting experimental arrangement for this experiment in which points of intersection of lines are measurement points. The dosimetry system used in these measurements was calibrated against secondary standard dosimetry system of SSDL, PINSTECH, Pakistan. The calibration factor ($N_{D,W}$) in charge mode turned out to be 48.88 mGy/μC. The corrected absorbed dose to water was determined using the following relation:

$$D_w = x \cdot k_{p,t} \cdot N_{D,W}$$

where x, $k_{p,t}$ and $N_{D,W}$ are uncorrected charge values, pressure temperature correction factor and chamber calibration factor, respectively. The $k_{p,t}$ is calculated as:

$$k_{p,t} = \frac{(T_m + 273.15) \times P_0}{(T_0 + 273.15) \times P_m}$$

where $P_0 = 1013.25$ mbar and $T_0 = 293.15$ K. P_m and T_m are average values of pressure and temperature, respectively, measured during the experiment.[14]

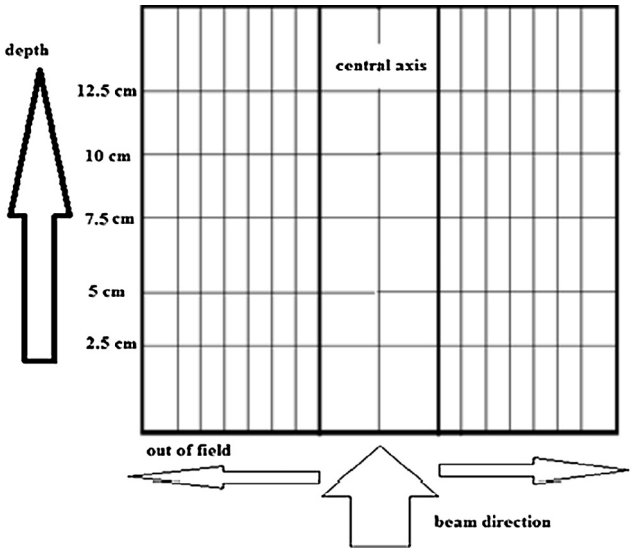

Fig. 1 – Experimental arrangement.

3. Results and discussion

In our study we considered location of tumour at six depths below the front surface of water phantom, 2.5–15 cm with an interval of 2.5 cm. For each field size, the variation of peripheral dose with lateral distance, from 1 cm to 6 cm, on both sides of the central beam axis was observed at each depth. All readings were normalized with respect to central beam axis dose at each location of tumour.

3.1. *Variation of central axis dose with depth*

Fig. 2 shows variation of central axis dose with depth along the beam axis. It is obvious that for a fixed field size, central axis dose decreases with depth because of photon beam attenuation and as a result of a decrease in forward scattering of electrons with increasing depth. It can be noticed that

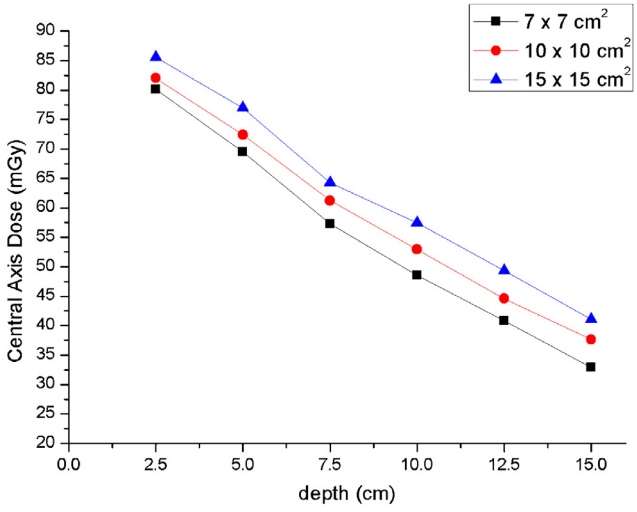

Fig. 2 – Variation of central axis dose with field size and depth.

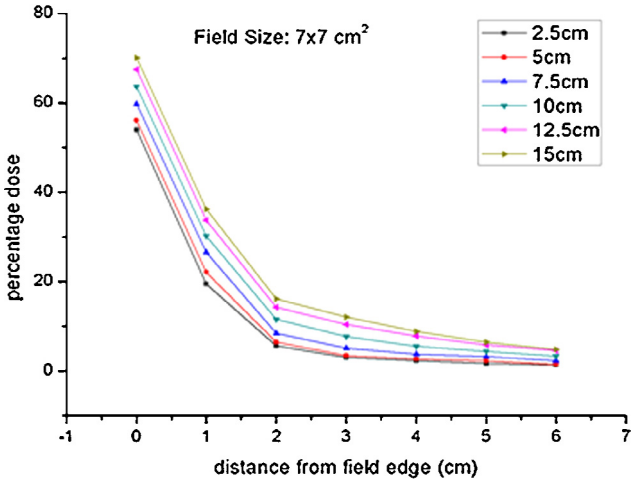

Fig. 3 – Dependence of peripheral dose on lateral axis distance.

this decrease is linear for each of the three field sizes. For the $10 \times 10\,cm^2$ field size, central axis dose varies from 82.04 mGy at 2.5 cm depth to 37.63 mGy at 15 cm depth. For the $7 \times 7\,cm^2$ and $15 \times 15\,cm^2$ field sizes, similar trend is observed. These results also show that there is a slight increase in central axis depth dose with increase in field size. This may be because of a slight increase in forward scattering of electrons with field size.[15]

3.2. *Peripheral dose variation with lateral distance*

From Fig. 3 it is clear that doses, outside the field boundary, decrease exponentially with increasing lateral distance (from boundary 0 cm to 6 cm) for a given field size at each depth. At 2.5 cm depth, peripheral dose varies from 56% at field boundary (0 cm) to 1.6% (of central beam dose) at 6 cm from the field edge. On the other hand, it varies from 75.3% at field boundary to 7.5% at 6 cm transverse distance from the field boundary for the depth of 15 cm.

McParland et al.[6] and Francois et al.[9] worked on a theoretical relationship for this dose fall off. In present study, an empirical equation was worked on. By fitting an equation to the data of dose for every depth, it is found that the following equation can be fit to each depth for any field size.

$$D(x) = Ae^{-x/t} + y_0$$

where 'x' is lateral distance from the field edge which ranges from 0 to 6 cm, A, t and y_0 are constants which are the functions of depth and field size themselves.

$$A = A(f, d)$$

$$t = t(f, d)$$

$$y_0 = y_0(f, d)$$

where f is the field size and d is depth in water phantom.

By fixing the field size, these constants will become a function of depth only. By plotting these constants with depth (d), following equations best fit to the curve for A, t and y_0.

$$A = \alpha_0 + \alpha_1 d$$

$$t = \tau_0 + \tau_1 d$$

For $7 \times 7\,cm^2$ and $10 \times 10\,cm^2$,

$$y_0 = \sigma_0 + \sigma_1 d + \sigma_2 d^2 + \sigma_3 d^3$$

In case of $15 \times 15\,cm^2$,

$$y_0 = \sigma_0 + \sigma_1 d + \sigma_2 d^2 + \sigma_3 d^3 + \sigma_4 d^4$$

Values of these constants are tabulated for $7 \times 7\,cm^2$, $10 \times 10\,cm^2$ and $15 \times 15\,cm^2$ field sizes in Table 1. This model was compared with experimental values and maximum observed deviations are 4% for $7 \times 7\,cm^2$, 7.17% for $10 \times 10\,cm^2$ and 7.48% for $15 \times 15\,cm^2$ field size. This difference was exhibited at such large lateral axis distances where dose is very low. Francois et al. showed a difference of less than 20% in his theoretical and experimental values at large distances from the central axis. At such large distances, these differences were not considered.[9]

This behaviour of peripheral dose may be due to the contribution of different components of scattered dose. Just outside the field boundary, scattering from within phantom is mainly responsible for the peripheral dose. As the distance from the field edge increases, phantom component of scatter dose rapidly reduces while the machine component (scattering from machine head, collimator jaws, etc.) increases. Near the field, both phantom scattering and collimator scattering are responsible for the peripheral dose but away from the field boundary only collimator scatter is accountable for peripheral dose.[9]

3.3. *Variation of peripheral dose with depth*

For a fix field size and lateral distance, dose outside field boundaries increases with increasing depth in a water phantom. For the $7 \times 7\,cm^2$ field size, dose at field boundary at depth of 2.5 cm is 53.97% of central axis dose. It increases with increasing depth and reaches 70.16% of central axis dose at 15 cm depth. At 1 cm lateral distance, it is 19.54% of central axis dose at 2.5 cm depth and increases to 36.29% central axis dose at 15 cm depth. Similar behaviour is exhibited for other lateral measurement points. Fig. 4 is a plot of peripheral doses against the depth for $7 \times 7\,cm^2$. It clearly shows an increase in peripheral dose with depth measured for every lateral axis measurement point. Similar behaviour is also exhibited for the field sizes of $10 \times 10\,cm^2$ and $15 \times 15\,cm^2$. Increase in peripheral dose follows a linear pattern. These results signify the fact that for deep seated tumours, scattered dose becomes more significant. In other words, dose to surrounding healthy tissues is higher in the case of deep seated tumours as compared with surrounding healthy tissues located at shallow depths.[10] Reason for this increase might be as follows: As photons penetrate deep inside the tissue, their energy decreases due to successive collisions with molecules of water. At low energies, photons predominantly scatter sideways in Compton

Table 1 – Values of constants for field sizes $7 \times 7\,cm^2$, $10 \times 10\,cm^2$ and $15 \times 15\,cm^2$.

$F \times S$ (cm^2)	α_0	α_1	τ_0	τ_1	σ_0	σ_1	σ_2	σ_3	σ_4
7×7	50.25	1.03	0.825	0.031	2.58	−0.85	0.14	−0.005	–
10×10	53.3	1.22	0.76	0.056	−0.23	0.87	−0.076	0.003	–
15×15	54.97	1.71	0.716	0.077	6.30	6.80	1.5	0.13	0.0039

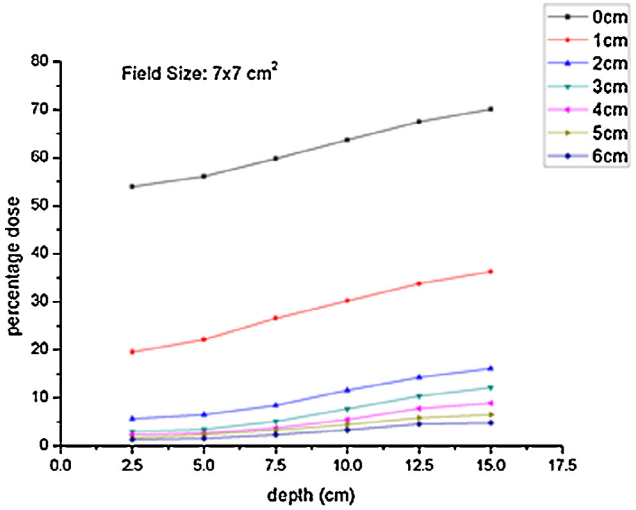

Fig. 4 – Variation of peripheral dose with depth.

scattering. This increases the absorbed dose outside the primary beam.

3.4. *Variation of peripheral dose with field size*

Fig. 5 shows peripheral doses at 2.5 cm depth for three field sizes. It is obvious that peripheral dose linearly increases with field size. At 1 cm from field edge, it is 22.14%, 25% and 32% of central beam axis dose at 5 cm for each field size, respectively, for the $7 \times 7\,cm^2$, $10 \times 10\,cm^2$ and $15 \times 15\,cm^2$ field sizes. The same distribution repeats for other depths with, obviously, a linear increase in doses for higher depths. This increase in field size may be due to the fact that a larger field size means more scattering centres for primary photons. More scattering of primary beam contributes to increased scattered dose.[6]

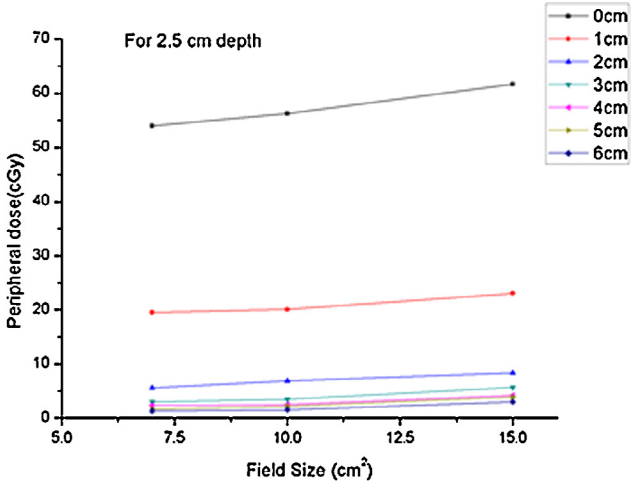

Fig. 5 – Variation of peripheral dose with field size.

3.5. *Error analysis*

Type-A uncertainties (statistical fluctuations in measurements) were calculated as deviation of right and left measurements relative to their mean value. Type-B uncertainties correspond to inherent errors in measuring instruments. This uncertainty was incorporated to the dosimetry system, thermometer and barometer. Uncertainties in positioning of the phantom and electrometer placed in water are ignored because the phantom is placed using a built-in scale and laser alignment system while the electrometer is placed in the water phantom using an inserter which has holes in it and is positioned at a fixed place.

Total Type-B uncertainty in measurement turned out to be ±0.9 cGy with a 95% confidence level.

4. Conclusion

Results of this study completely agree with previous studies[1–12] and the proposed mathematical model has been suggested for peripheral dose. Peripheral dose is an important consideration when delivering radiation doses to patients with megavoltage photon beams. It can cause higher than anticipated doses to OARs. Choice of field size during radiotherapy planning has to be optimized so as to minimize scattered dose to the organs outside treatment area. The presented work can be extended for tissue composition by introducing density parameter to the proposed mathematical model. The resultant equation can be used as a simulation tool for radiotherapy treatment planning.

Conflict of interest

None declared.

Financial disclosure

This research was carried out as requirement for MS degree completion. All funding was given by Pakistan Institute of Engineering and Applied Sciences Islamabad, Pakistan.

Acknowledgements

All the praise for Allah Almighty – The CREATOR of the worlds – for giving me the respect and nobility more than I deserve. Gratitude and Admiration to Prophet Muhammad (Peace Be

Upon Him), who is the ultimate role model for all the humanity.

I would like to thank Mr. Asadullah (SS) and Dr. Wazir Hussain for the moral support and encouragement during my stay at SSDL-HPD. Spacial thanks to Mr. Zia Khursheed and Mr. Anees Farooqi for their cooperation in experimental work for this article.

REFERENCES

1. Cigna AA, Nassisi D, Masenga D, Raffo R, Rotta P. Dose due to scattered radiation in external radiotherapy: a prostate ccancer case history. *Radiat Prot Dosimetry* 2004;**108**:27–32.
2. Fraass BA, van de Geijn J. Peripheral dose from megavolt beams. *Med Phys* 1983;**10**:809–18.
3. Starkschall G, St George FJ, Zellmer DL. Surface dose for mega voltage photon beams outside the treatment field. *Med Phys* 1983;**10**:906–10.
4. Diallo I, Lamon A, Shamsaldin A, Grimaud E, de Vathaire F, Chavaudra J. Estimation of the radiation dose delivered to any point outside the target volume per patient treated with external beam radiotherapy. *Radiother Oncol* 1996;**38**:269–71.
5. Garth JC, Burke EA, Woolf S. The role of scattered radiation in the dosimetry of small device structures. *IEEE Trans Nucl Sci* 1980;**NS-27**:1459–64.
6. McParland Brian J, Fair HI. A method of calculating peripheral dose distributions of photon beams below 10 MV. *Med Phys* 1992;**19**:283–93.
7. Van der Giessen P-H. A simple and generally applicable method to estimate the peripheral dose in radiation teletherapy with high energy X-rays or gamma radiation. *Int J Radiat Oncol Biol Phys* 1996;**35**:1059–68.
8. Van der Giessen P-H. Measurement of the peripheral dose for the tangential breast treatment technique with Co-60 gamma radiation and high energy X-rays. *Radiother Oncol J* 1997;**8140**.
9. Francois P, Beurtheret C, Dutreix A. Calculation of the dose delivered to organs outside the radiation beams. *Med Phys* 1988;**15**:879–83.
10. Rafiuddin M, Alam MJ, Ahmad GU. Measurement of dose out side the irradiated volume by using locally fabricated water phantom. *Bangladesh J Med Phys* 2003;**2**:41–4.
11. Arshad W, Akhter P, Ullah A, et al. Assessment of scatter dose contribution to healthy tissue in radiotherapy using water phantom. *Nucl Technol Radiat Prot* 2010;**25**:212–6.
12. Mutic S, Esthappan J, Klein EE. Peripheral dose distributions for a linear accelerator equipped with a secondary multileaf collimator and universal wedge. *J Appl Clin Med Phys* 2002;**3**:302–9.
13. Balasubramanian R, Sellakumar P, Bilimagga RS, Supe SS. Measurements of peripheral dose for multileaf collimator based linear accelerator. *Rep Pract Oncol Radiother* 2006;**11**:281–5.
14. IAEA. *TRS-398 absorbed dose determination in external beam radiotherapy*; 2000.
15. Khan FM. *Physics of radiation therapy*. Lippincott Williams & Wilkins; 2010.